

**Pressure-induced phase transitions in iron-filled carbon nanotubes: X-ray diffraction studies**Sukanta Karmakar,<sup>1</sup> Surinder M. Sharma,<sup>1</sup> P. V. Teredesai,<sup>2</sup> and A. K. Sood<sup>2,3</sup><sup>1</sup>*Synchrotron Radiation Section, Bhabha Atomic Research Centre, Mumbai 400085, India*<sup>2</sup>*Department of Physics, Indian Institute of Science, Bangalore 560012, India*<sup>3</sup>*Chemistry and Physics of Materials Unit, Jawaharlal Nehru Centre for Advanced Scientific Research Centre, Jakkur Campus, Jakkur, Bangalore 560 064, India*

(Received 8 September 2003; revised manuscript received 12 January 2004; published 27 April 2004)

High-pressure x-ray-diffraction studies have been carried out upto 20 GPa on iron-filled multiwalled carbon nanotubes (MWNTs). The pressure dependence of the intertubular spacing  $d_0$  of the filled MWNTs shows a sharp change at 9 GPa which is not observed in pristine MWNTs. The iron present as nanowires inside the MWNT is in the form of  $\alpha$ -Fe and  $\text{Fe}_3\text{C}$ . Both of these phases show higher compressibility than their bulk form. Most interestingly, the structural modification of MWNTs at 9 GPa coincides with an iso-structural phase transition in the encapsulated  $\text{Fe}_3\text{C}$ , in sharp contrast to the absence of a transition in the bulk  $\text{Fe}_3\text{C}$  upto 70 GPa.

DOI: 10.1103/PhysRevB.69.165414

PACS number(s): 61.46.+w

**INTRODUCTION**

Carbon nanotubes are amongst the most exciting new materials being investigated because of their potential uses in new technologies and devices exploiting their unusual mechanical and electrical properties.<sup>1,2</sup> In particular, multiwall carbon nanotubes (MWNTs) are of interest to the growing microfluidic and nanofluidic industry.<sup>3</sup> These MWNTs are composed of several concentric cylindrical graphene tubules, with an intertube separation  $d_0$  of  $\sim 3.4$  to  $3.9$  Å, which increases with decreasing radii.<sup>4</sup> Recently the synthesis of various metal filled carbon nanotubes has also been achieved successfully.<sup>5–8</sup> There have been a number of theoretical and experimental studies related to elasticity, strength, and toughness of MWNTs.<sup>9–14</sup> High-pressure x-ray-diffraction experiments on pristine MWNTs show that these nanotubes become partly amorphous when compressed above 8 GPa.<sup>15</sup> In addition, recent Raman scattering investigations on MWNTs show a small change in slope of the high-frequency tangential modes at  $\sim 1$  GPa, which has been attributed to the reversible flattening of the nanotubes.<sup>16</sup> While the metal filling does not significantly change shape and size of the nanotubes, it can affect the mechanical properties significantly. Molecular dynamics simulations<sup>17</sup> have shown that the buckling force of single-walled carbon nanotubes (SWNTs) is increased when filled with  $\text{C}_{60}$ ,  $\text{CH}_4$ , and Ne. However, there is no high-pressure experimental study so far to understand the effect of filling on the elastic properties and stability of single-walled as well as multiwalled carbon nanotubes. In addition, such experiments will also help to understand the high pressure behavior of the nanocrystalline metallic wires or particles which are formed inside the nanotubes. With a view to understand the effect of metal filling on MWNTs, we have carried out high-pressure angle dispersive x-ray-diffraction experiments on pure and Fe-filled MWNT. A sharp change is seen in the intertubular distance  $d_0$  in Fe-filled MWNTs at  $\sim 9$  GPa, in sharp difference to the pristine MWNTs. Encapsulated iron in the nanotubes is in the form of  $\alpha$ -Fe and  $\text{Fe}_3\text{C}$ .<sup>7,18</sup> The pressure behavior of these

nanocrystalline forms of  $\alpha$ -Fe and  $\text{Fe}_3\text{C}$  are investigated and are shown to be very different from their bulk counter parts.

**EXPERIMENTAL DETAILS**

Fe-filled multiwall carbon nanotubes prepared by pyrolysis of ferrocene along with acetylene using a two-stage furnace are same as described in Ref. 7. TEM studies show the presence of nanowires encapsulated inside carbon nanotubes.<sup>7</sup> High-resolution electron microscope image (Fig. 2 of Ref. 7) shows that there is no free space between the metal nanowire and the carbon nanotube. The nanowires show a distribution in their diameter and length, the diameter being in the range of 10–20 nm and the length in the 200–800 nm range. In addition to the nanowires, a small portion of iron nanoparticles, with 20–40 nm diameter, covered with graphite layer were also found.

For the purpose of high pressure experiments Fe-filled MWNTs (along with a few specs of gold) were loaded in a hole of  $\sim 120$   $\mu\text{m}$  diameter drilled in a preindented ( $\sim 70$  micron) steel gasket of a Mao-Bell kind diamond-anvil cell (DAC). Methanol:ethanol:water(16:3:1) mixture was used as pressure transmitting medium which provides hydrostatic pressure environment until  $\sim 15$  GPa. The pressure was determined from the known equation of state of gold.<sup>19</sup> High-pressure angle dispersive x-ray-diffraction experiments, were carried out up to  $\sim 20$  GPa, at the 5.2 R beamline of Elettra Synchrotron source with monochromatized x rays ( $\lambda = 1.0$  Å). The diffraction patterns were recorded using MAR345 imaging plate detector kept at a distance of  $\sim 21$  cm from the sample. Two-dimensional imaging plate records were transformed to one-dimensional diffraction profiles by the radial integration of diffraction rings using the FIT2D software.<sup>20</sup> Experiments on pure MWNTs were carried out using a laboratory x-ray-diffraction source (Mo  $K_\alpha$ ) along with an imaging plate and ruby pressure marker.

**RESULTS AND DISCUSSION**

Figure 1 shows the x-ray-diffraction profile of the iron filled multiwall carbon nanotubes at 0.3 GPa. The diffraction

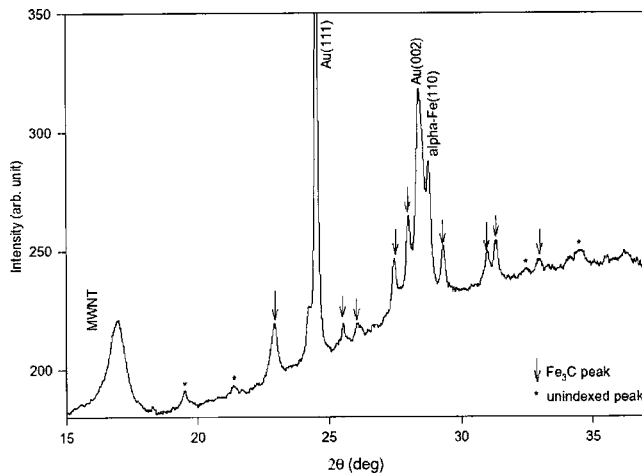


FIG. 1. X-ray diffraction profile of Fe-filled MWNTs at 0.3 GPa. The peak marked MWNT is the characteristic peak of the nanotube associated with the average intershell distance. Au(111) and Au(002) lines are used as pressure markers.  $\alpha$ -Fe(110) peak is the characteristic peak for the  $\alpha$ -iron phase. The peaks marked by arrows correspond to the  $\text{Fe}_3\text{C}$  phase. The peaks marked by stars are not indexed.

peak marked as MWNT is the characteristic peak for the multiwall carbon nanotubes representing the average intershell distance and gives intertubular spacing  $d_0 = 3.42 \text{ \AA}$ . The pattern covering  $2\theta$  from  $22^\circ$  to  $37^\circ$  can be analyzed very well<sup>21</sup> in terms of three components— $\alpha$ -Fe, orthorhombic  $\text{Fe}_3\text{C}$ , and fcc Au, with the help of the Reitveld refinement using GSAS software.<sup>22</sup> The relative proportions of  $\alpha$ -Fe and  $\text{Fe}_3\text{C}$  are found to be 80 and 19%, respectively, and the  $\gamma$ -Fe phase is less than 1%. Prados *et al.*<sup>18</sup> have suggested that inner  $\gamma$ -Fe core is surrounded, from inside to outside, by  $\gamma$ -Fe,  $\text{Fe}_3\text{C}$ , and carbon layers. The refined unit cell dimensions of  $\alpha$ -Fe (space group Im3m) is determined to be  $2.880 \pm 0.001 \text{ \AA}$  compared to  $2.87 \text{ \AA}$  of bulk  $\alpha$ -Fe. For  $\text{Fe}_3\text{C}$  (orthorhombic structure, space group Pnma) the unit cell parameters are  $a = 5.108 \pm 0.002 \text{ \AA}$ ,  $b = 6.826 \pm 0.003 \text{ \AA}$ ,  $c = 4.5680 \pm 0.002 \text{ \AA}$  (compare these with the values for bulk  $\text{Fe}_3\text{C}$ :  $a = 5.088 \pm 0.002 \text{ \AA}$ ,  $b = 6.742 \pm 0.003 \text{ \AA}$ ,  $c = 4.526 \pm 0.003 \text{ \AA}$ ). Larger values of lattice parameters of nanocrystalline  $\text{Fe}_3\text{C}$  compared to bulk is expected as the free surface in nanograins can be under tensile strain.<sup>23</sup> The refined fractional coordinates are given below (for bulk  $\text{Fe}_3\text{C}$  the corresponding values are given in the parenthesis<sup>24</sup>):

$$\text{Fe}(1): 0.076, 0.25, 0.827 \text{ (}0.036, 0.25, 0.840\text{)},$$

$$\text{Fe}(2): 0.242, 0.056, 0.350 \text{ (}0.182, 0.066, 0.337\text{)},$$

$$\text{C}: 0.813, 0.25, 0.562 \text{ (}0.877, 0.25, 0.444\text{)}.$$

Figure 2 shows the diffraction patterns of Fe-filled MWNTs at a few representative pressures. Before we discuss the behavior of nanocrystalline  $\alpha$ -Fe and  $\text{Fe}_3\text{C}$ , we focus on the stability of the MWNTs. The observed value of average  $d_0 = 3.42 \text{ \AA}$  at ambient pressures compares favourably with the values reported by other investigators<sup>4</sup> and its difference from  $d_{002}$  of graphite ( $3.353 \text{ \AA}$ ) has been interpreted as due

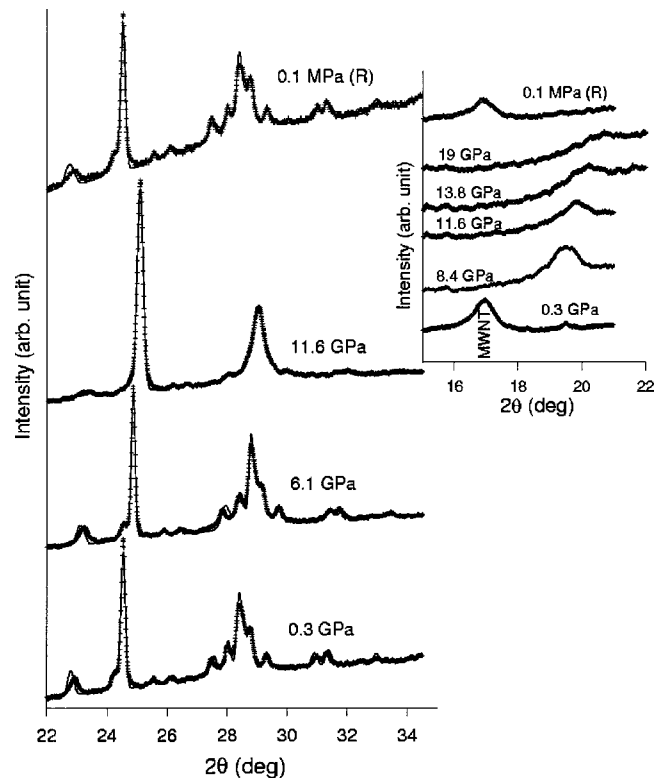


FIG. 2. Diffraction patterns of Fe-filled MWNTs at various pressures. (A break in the  $x$  axis at  $\sim 21^\circ$  is used to imply different intensity scales). Beyond  $22^\circ$ , the data is analyzed by Reitveld analysis and this is shown at (a) 0.3 GPa, (b) 6 GPa, (c) 11.6 GPa, and (d) 0.1 MPa released from 19 GPa. Displayed are the observed (dots) and calculated (lines) spectra. The inset shows the MWNT line at a few pressures.

to the curvature of the tubes. The asymmetric line shape of the MWNTs diffraction peak can be due to a distribution of intershell distances because  $d_0$  is known to decrease with the radii of the tubes.<sup>4</sup> Since the focus of the present paper is to address the high-pressure behavior of the Fe-filled tubes, we will view  $d_0$  to correspond to the average intershell separation. The asymmetric line shape was fitted to a sum of Gaussian and Lorentzian function, as usually done in the literature.<sup>25</sup> The variation of this intershell spacing  $d_0$  with pressure is shown in Fig. 3 for Fe-filled (filled triangles) and pristine MWNTs (filled circles) in increasing pressure runs. Also shown for comparison is the pressure variation of  $d_{002}$  of graphite (dotted line) generated<sup>26</sup> using bulk modulus  $B = 35.7 \text{ GPa}$ , its pressure derivative  $B' = 10.8$  in one-dimensional Murnaghan equation  $a/a_0 = [(B'/B)P + 1]^{-1/B'}$ . The results for decreasing pressure for Fe-filled MWNTs are also shown by open triangles. The inset shows the full width at half maximum  $\Gamma$  of the MWNT diffraction line for the filled tubes. It can be seen that there is a sharp increase in  $\Gamma$  beyond 9 GPa, a feature similar to what has been observed for the pristine tubes and has been ascribed to partial disorder.<sup>15</sup> Alternatively, this could also be due to heterogeneous deformation of the tubes. Based on our data, the following observations can be made. (1) The  $d_0$  value at low pressure ( $P < 0.3 \text{ GPa}$ ) for Fe-filled tubes ( $d_0 = 3.42 \text{ \AA}$ ) is

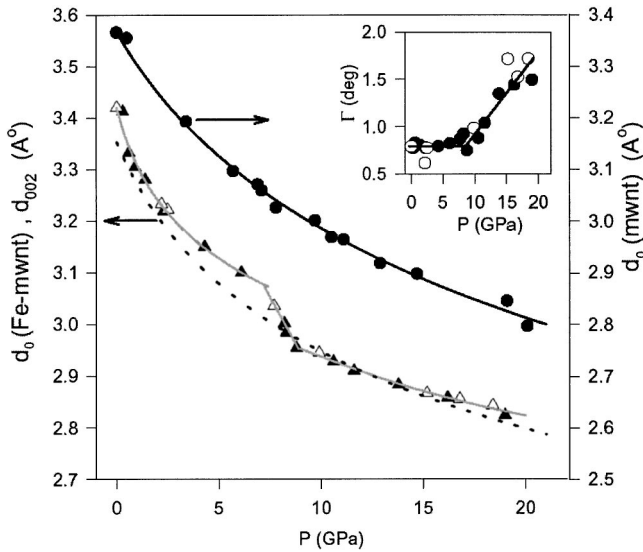


FIG. 3. Variation of the average intershell distance  $d_0$  with pressure for (solid triangles for increasing pressure and open triangles for decreasing pressure), and for pristine MWNT (solid circle). Variation of  $d_{002}$  line of graphite (dash line) is also plotted for comparison. For the sake of clarity of presentation, the left side y axis is for the filled tubes and graphite, whereas the right side is for pristine tubes. The inset shows variation of the line width of the MWNT diffraction line for iron filled MWNT.

slightly larger than that in pristine MWNTs ( $d_0=3.37 \text{ \AA}$ ). (2) The  $d_0$  value shows a sharp decrease at  $\sim 9 \text{ GPa}$  for Fe-filled tubes, whereas no such changes are seen in the case of pristine tubes. A simple geometric analysis indicates that polygonization of tubes leads to a reduction in intershell separation. For example, for hexagonal deformation, the reduction is by a factor of  $\sim 0.9$ . Therefore, a probable explanation of the drop in  $d_0$  at 9 GPa could be in terms of polygonization or ovalization of the tubes' cross section, as observed also in single-wall carbon nanotubes.<sup>27</sup> The transi-

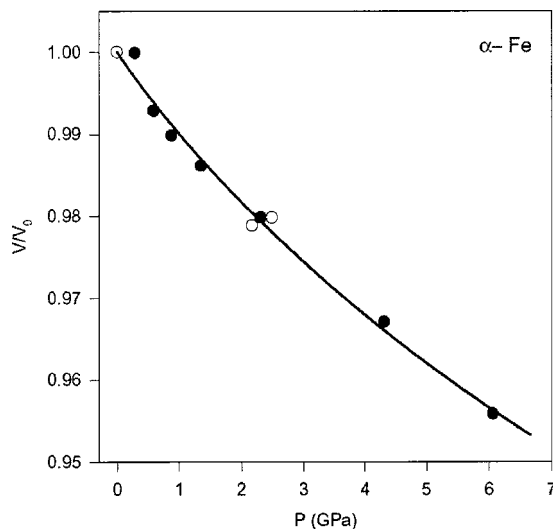


FIG. 4. Volume compression  $V/V_0$  of nanocrystalline  $\alpha$ -Fe present inside the nanotube as a function of pressure. The solid line is a fit to Murnaghan equation.

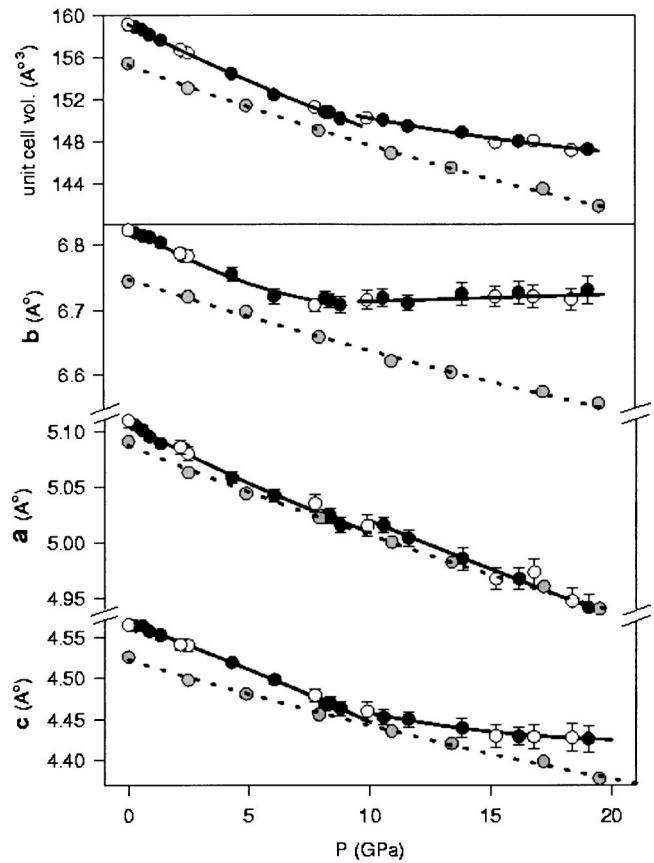


FIG. 5. Variation of cell parameters and unit cell volume of  $\text{Fe}_3\text{C}$  as a function of pressure. Filled gray circles represent bulk  $\text{Fe}_3\text{C}$  (from Ref. 32). Solid and dotted lines are the quadratic fits to our and the data from Ref. 32, respectively.

tion pressure of 9 GPa seen in our experiments is much lower than the pressure of 15 GPa when the pressure transmitting medium freezes and hence the nonhydrostaticity cannot be the reason for observing the changes in  $d_0$  and  $\Gamma$ . (3) Up to  $\sim 7 \text{ GPa}$ , the pressure variation of the  $d_0$  is same for pristine as well as filled tubes. When fitted to one-dimensional Murnaghan equation<sup>26</sup> we get  $B=49.3 \text{ GPa}$  and  $B'=8.1$ . Therefore, MWNTs, similar to SWNTs<sup>27</sup> are less compressible than graphite.<sup>4</sup> Beyond 9 GPa, the  $d_0$  for filled MWNTs is same as  $d_{002}$  of graphite. We point out that the diffraction lines got weaker beyond 9 GPa, and therefore, the errors in  $d_0$  are somewhat larger than below 9 GPa.

The high-pressure behavior of  $\alpha$ -Fe formed inside the encapsulated iron nanowires is presented in Fig. 4. As the observed diffraction peaks are very weak beyond  $\sim 6 \text{ GPa}$ , the data is analyzed only upto this pressure. When fitted to Murnaghan equation of state, we get  $B=89.7 \pm 9.4 \text{ GPa}$  with  $B'=20.9 \pm 7$ . These results suggest that  $\alpha$ -Fe in the nanocrystalline form is roughly twice more compressible than the bulk  $\alpha$ -Fe ( $B=169.8 \text{ GPa}$ ). This is similar to the observation of sixfold enhancement in compressibility of the nanocrystalline  $\alpha$ -Fe seen in a low-pressure Mossbauer study ( $< 1 \text{ GPa}$ ).<sup>28</sup> The increased compressibility is attributed to the lower effective elastic constants of intercrystalline regions surrounding the nanometer sized crystals and forming a net-

work between them. We should also note that  $\alpha$ -Fe in MWNTs does not undergo bcc-hcp phase transformation up to 20 GPa, while in the bulk this phase transformation takes place at  $\sim 14$  GPa.<sup>29</sup> However, an increase in the transformation pressure in nanocrystalline materials compared to the bulk has also been observed in other materials.<sup>30</sup>

As mentioned above, Reitveld profile analysis shows that nanocrystalline Fe<sub>3</sub>C present in nanotubes has a larger unit cell as well as the atomic arrangement is different from that in the corresponding bulk phase. The diffraction pattern associated with Fe<sub>3</sub>C can be well refined with the space group Pnma up to the maximum pressure in the present study. Figure 5 show the pressure variation of the cell parameters and the unit cell volume. The filled dark (open) circles correspond to increasing (decreasing) pressure runs. The solid lines are fit to a quadratic equation. The cell constants **a** decreases systematically up to 9 GPa and then shows a upward jump followed by a smooth decrease up to the maximum pressure. In contrast, **b** reduces up to 9 GPa and thereafter the variation is small. The cell constant **c** also shows a change in slope at  $\sim 9$  GPa. The pressure-volume curve in Fig. 5 also shows a clear signature of a phase transition at 9 GPa. An accurate analysis of pressure-induced variation in the fractional coordinates is rendered difficult due to the reduction in the diffracted intensity. However, the results do suggest some atomic rearrangements at  $\sim 9$  GPa. These results clearly suggest a possibility of an isostructural phase transition in nanocrystalline Fe<sub>3</sub>C at  $\sim 9$  GPa, the pressure at which the intertube spacing  $d_0$  of MWNTs also shows a sharp reduction. Interestingly, this is in sharp contrast to the behavior of bulk Fe<sub>3</sub>C which shows no phase transition up to 73 GPa.<sup>31</sup> This is clearly depicted by the data<sup>32</sup> for bulk Fe<sub>3</sub>C shown by gray filled circles in Fig. 5. As no phase transformation is observed either in pristine tubes or bulk Fe<sub>3</sub>C at  $\sim 9$  GPa, it is difficult to ascertain whether the nanocrystalline Fe<sub>3</sub>C or the filled MWNTs drive the transformation. However, an independent study of nanocrystalline Fe<sub>3</sub>C will help to resolve this issue. We also note that no sudden change is observed in  $\alpha$ -Fe at this pressure. The  $P$ - $V$  data of nanocrystalline Fe<sub>3</sub>C, when fitted using Murnaghan equation of state up to 9 GPa gives the bulk modulus  $B=135$

$\pm 4$  GPa and its pressure derivative  $B'=4.05\pm 1$ , which is considerably smaller than reported previously for bulk Fe<sub>3</sub>C ( $B=175\pm 4$  GPa and  $B'=5.2\pm 0.3$ ).<sup>31,32</sup> This again establishes that nanocrystalline materials can have a higher compressibility than their bulk counterparts. However, our results on Fe<sub>3</sub>C imply that the behavior of nanocrystalline phase encapsulated in MWNTs is different from normal nanophase material. In addition, one cannot just suppose that the deformation of MWNT triggers phase transformation as that is not observed in  $\alpha$ -Fe. Moreover, homogeneous deformation theories<sup>30</sup> suggest that the smaller dimensions of the nanoparticles result in increase of pressure of transformation, which is at variance with our results in Fe<sub>3</sub>C. Therefore, the present results should encourage more experimental and theoretical work to unravel the underlying particle-tube interactions, which bring out the observed differences.

To summarize, the nanowires of iron formed in the MWNTs have two phases— $\alpha$ -Fe and Fe<sub>3</sub>C. Both  $\alpha$ -Fe and Fe<sub>3</sub>C in the nanocrystalline form synthesized inside the nanotubes are shown to be more compressible than the corresponding bulk material. The filled MWNTs, unlike pure MWNTs, undergo a structural modification at  $\sim 9$  GPa as shown by a sharp reduction in the intertube separation, an increase in  $\Gamma$  as well as in the decrease of the diffraction intensity. This structural change in MWNTs is coincident with an isostructural phase transformation in Fe<sub>3</sub>C at  $\sim 9$  GPa. It will be interesting to study theoretically what drives the pressure-induced transitions in MWNTs as well as in Fe<sub>3</sub>C.

## ACKNOWLEDGMENTS

X-ray diffraction experiments were performed at 5.2R powder x-ray diffraction beamline of Elettra, Italy. Proposal No. 2001049. We thank the Department of Science and Technology, Government of India, for financial assistance. A.K. Sood thanks Professor C.N.R. Rao and Dr. A. Govindaraj for fruitful interactions and the samples and S. Karmakar and S. M. Sharma thank Dr. S. K. Sikka for his valuable suggestions.

<sup>1</sup>C. N. R. Rao, B. C. Satishkumar, A. Govindaraj, and M. Nath, *ChemPhysChem* **2**, 78 (2001).

<sup>2</sup>P. J. F. Harris, *Carbon Nanotubes and Related Structures: New Materials for the Twenty First Century* (Cambridge University Press, Cambridge, 1999).

<sup>3</sup>M. A. Burns, B. N. Johnson, S. N. Brahmasandra, K. Handique, J. R. Webster, M. Krishnan, T. S. Sammarco, P. M. Man, D. Jones, D. Heldsinger, C. H. Mastrangelo, and D. T. Burke, *Science* **282**, 484 (1998).

<sup>4</sup>C. H. Kinag, M. Endo, P. M. Ajayan, G. Dresselhaus, and M. S. Dresselhaus, *Phys. Rev. Lett.* **81**, 1869 (1998).

<sup>5</sup>P. M. Ajayan and S. Iijima, *Nature (London)* **361**, 333 (1993).

<sup>6</sup>R. S. Ruoff, D. C. Lorents, B. Chan, R. Malhotra, and S. Subramoney, *Science* **259**, 346 (1993).

<sup>7</sup>B. C. Satishkumar, A. Govindaraj, P. V. Vanitha, A. K. Raychaudhuri, and C. N. R. Rao, *Chem. Phys. Lett.* **362**, 301 (2002).

<sup>8</sup>X. Ma, Y. Cai, N. Lun, Q. Ao, S. Li, F. Li, and S. Wen, *Mater. Lett.* **4258**, 1 (2002).

<sup>9</sup>E. W. Wong, P. E. Sheehan, and C. M. Lieber, *Science* **277**, 1971 (1997).

<sup>10</sup>Min-Feng Yu, O. Lourie, M. J. Dyer, K. Moloni, T. F. Kelly, and R. S. Ruoff, *Science* **287**, 637 (2000).

<sup>11</sup>C. Q. Ru, *J. Appl. Phys.* **89**, 3426 (2001).

<sup>12</sup>B. A. Galanov, S. B. Galanov, and Y. Gogotsi, *J. Nanopart. Res.* **4**, 207 (2002).

<sup>13</sup>Zhan-chun Tu and Zhong-can Ou-Yang, *Phys. Rev. B* **65**, 233407 (2002).

<sup>14</sup>C. Wei, K. Cho, and D. Srivastava, *Appl. Phys. Lett.* **82**, 2512

- (2003).
- <sup>15</sup>C. Liang-Chang, W. Li-Jun, T. Dong-Sheng, X. Si-Shen, J. Chang-Qing, *Chin. Phys. Lett.* **18**, 577 (2001).
- <sup>16</sup>J. Sandler, M. S. P. Shaffer, A. H. Windle, M. P. Halsall, M. A. Montes-Moran, C. A. Copper, and R. J. Young, *Phys. Rev. B* **67**, 035417 (2003).
- <sup>17</sup>B. Ni, S. B. Sinnott, P. T. Mikulski, and J. A. Harrison, *Phys. Rev. Lett.* **88**, 205505-1 (2002).
- <sup>18</sup>C. Prados, P. Crespo, J. M. Gonzalez, A. Hernando, J. F. Marco, R. Gancedo, N. Grobert, M. Terrones, R. M. Walton, and H. W. Kroto, *Phys. Rev. B* **65**, 113405 (2002).
- <sup>19</sup>D. L. Heinz and R. Jeanloz, *J. Appl. Phys.* **55**, 885 (1984).
- <sup>20</sup>A. P. Hammersley, S. O. Svensson, M. Hanfland, A. N. Fitch, and D. Hauserman, *High Press. Res.* **14**, 235 (1996).
- <sup>21</sup>Typical value for fit are  $\chi^2 < 0.05$ ,  $R(p) < 1.0\%$ ,  $R(wp) < 1.5\%$ .
- <sup>22</sup>A. C. Larson, R. B. Von Dreele, *GSAS: general structure analysis system*. Los Alamos National Laboratory LAUR Publication, 1998.
- <sup>23</sup>B. Palosz, S. Gierlotka, S. Stel'makh, R. Pielaszele, P. Zinn, M. Winzenick, U. Bismayer, and H. Boysen, *J. Alloys Compd.* **286**, 184 (1999).
- <sup>24</sup>E. J. Fasiska and G. A. Jeffrey, *Acta Crystallogr.* **19**, 463 (1965).
- <sup>25</sup>D. Louer, in *Powder Diffraction*, edited by S. P. Sen Gupta and P. Chatterjee (Allied Publisher, New Delhi, 2002), pp. 1–16.
- <sup>26</sup>M. Hanfland, H. Beister, and K. Syassen, *Phys. Rev. B* **39**, 12 598 (1989).
- <sup>27</sup>S. M. Sharma, S. Karmakar, S. K. Sikka, P. V. Teredesai, A. K. Sood, A. Govindaraj, and C. N. R. Rao, *Phys. Rev. B* **63**, 205417 (2001).
- <sup>28</sup>S. Trapp, C. T. Limbach, U. Gonser, S. J. Campbell, and H. Gleiter, *Phys. Rev. Lett.* **75**, 3760 (1995).
- <sup>29</sup>R. Boehler, N. Vonbargen, and A. Chopelas, *J. Geophys. Res. B* **95**, 21731 (1990).
- <sup>30</sup>Sarah H. Tolbert, Amy B. Herhold, Louis E. Brus, and A. P. Alivisatos, *Phys. Rev. Lett.* **76**, 4384 (1996); Juanita N. Wickham, Amy B. Herhold, and A. P. Alivisatos, *ibid.* **84**, 923 (2000).
- <sup>31</sup>H. P. Scott, Q. Williams, and E. Knittle, *Geophys. Res. Lett.* **28**, 1875 (2001).
- <sup>32</sup>J. Li, H. K. Mao, Y. Fei, E. Gregoryanz, M. Eremets, and C. S. Zha, *Phys. Chem. Miner.* **29**, 166 (2002).